Nonuniform Elasticity of Titin in Cardiac Myocytes: A Study Using Immunoelectron Microscopy and Cellular Mechanics

Henk Granzier, Michiel Helmes, and Károly Trombitás

Department of Veterinary and Comparative Anatomy, Pharmacology, and Physiology, Washington State University, Pullman, Washington 99164 USA

ABSTRACT Titin (also known as connectin) is a muscle-specific giant protein found inside the sarcomere, spanning from the Z-line to the M-line. The I-band segment of titin is considered to function as a molecular spring that develops tension when sarcomeres are stretched (passive tension). Recent studies on skeletal muscle indicate that it is not the entire I-band segment of titin that behaves as a spring; some sections are inelastic and do not take part in the development of passive tension. To better understand the mechanism of passive tension development in the heart, where passive tension plays an essential role in the pumping function, we investigated titin's elastic segment in cardiac myocytes using structural and mechanical techniques. Single cardiac myocytes were stretched by various amounts and then immunolabeled and processed for electron microscopy in the stretched state. Monoclonal antibodies that recognize different titin epitopes were used, and the locations of the titin epitopes in the sarcomere were studied as a function of sarcomere length. We found that only a small region of the I-band segment of titin is elastic; its contour length is estimated at ~75 nm, which is only ~40% of the total I-band segment of titin. Passive tension measurements indicated that the fundamental determinant of how much passive tension the heart develops is the strain of titin's elastic segment. Furthermore, we found evidence that in sarcomeres that are slack (length, ~1.85 μm) the elastic titin segment is highly folded on top of itself. Based on the data, we propose a two-stage mechanism of passive tension development in the heart, in which, between sarcomere lengths of ~1.85 μm and ~2.0 μm, titin's elastic segment straightens and, at lengths longer than ~2.0 μm, the molecular domains that make up titin's elastic segment unravel. Sarcomere shortening to lengths below slack (~1.85 μm) also results in straightening of the elastic titin segment, giving rise to a force that opposes shortening and that tends to bring sarcomeres back to their slack length.

INTRODUCTION

When a passive muscle is stretched it develops passive tension. Passive tension opposes the stretch and restores the original length of the muscle after release. In contrast to active tension, which is known to be based on actomyosin interaction, the nature and underlying mechanism of passive tension are not well understood. A giant protein (M_r of approximately three million), known both as titin and connectin, has recently been described in skeletal and cardiac muscles; the sarcomere location and the molecular properties of this protein suggest that it provides the molecular basis for passive tension (for reviews see Wang, 1985; Maruyama, 1986, 1994; Trinick, 1991; Fulton and Isaacs, 1991). Skeletal muscle titin has been studied by measuring at a range of sarcomere lengths the position of monoclonal titin antibodies that label different epitopes along the molecule (Itoh et al., 1988; Fürst et al., 1988; Whiting et al., 1989; Pierobon-Bormioli et al., 1989; Horowits et al., 1989; Trombitás et al., 1991; Wang et al., 1991, 1993). These studies have revealed that a single titin molecule extends from the Z-line to the M-line of the sarcomere, a distance of ~1–2 μm. Furthermore, the titin segment in the I-band was found to be extensible, whereas the segment in the A-band was not. The I-band segment of titin has been proposed to function as a molecular spring that develops a restoring force upon sarcomere stretch, a force that underlies passive tension (Wang, 1985; Maruyama, 1986, 1994). The hypothesis that titin plays a role in passive tension generation was supported by studies in which passive tension was reduced significantly after the degradation of titin by either ionizing radiation (Horowits et al., 1986) or digestion by trypsin (Yoshioka et al., 1986; Higuchi, 1992; Granzier and Irving, 1995). Thus, the sarcomeric location and elastic nature of titin makes it the ideal candidate for providing the molecular basis for passive tension.

Although the entire I-band segment of skeletal muscle titin is generally assumed to be elastic, recent studies indicate that some of its sections are inelastic. The studies of Fürst et al. (1988), Trombitás et al. (1991), and Trombitás and Pollack (1993) have revealed that, in skeletal muscle, the 100-nm-long titin segment adjoining the Z-line and the 50-nm-long segment adjoining the A/I junction are inelastic. Thus, in skeletal muscle, the elastic segment of titin, and hence the segment that develops passive tension, is much shorter than the width of the I-band.

Most of our knowledge about titin and passive tension is obtained from studies using skeletal muscle. However, passive tension is more fundamentally important in the heart where it contributes to the diastolic wall tension, a factor that determines the heart's extent of filling and subsequent stroke volume. In recent studies evidence was found that a

considerable fraction of the passive tension developed by the heart is titin based (Brady, 1991; Linke et al., 1994; Granzier and Irving, 1995). Furthermore, we showed that the increase of titin-based tension with sarcomere length is much steeper than in skeletal muscle (Granzier and Irving, 1995). The steeper increase has been ascribed to the fact that the heart expresses a smaller titin size variant (~2.5 MDa) than skeletal muscle does (~3.0 MDa) and that this results in a larger strain of the I-band segment of titin for a given degree of sarcomere stretch (Granzier and Irving, 1995). However, to make such a comparison and to understand passive tension of the heart better, it is important to know the length of cardiac titin's elastic segment.

We investigated the elastic behavior of different segments of the titin molecule in cardiac muscle by using immunoelectron microscopy on single rat cardiac myocytes that had been stretched before labeling with several different monoclonal antibodies against titin. Our results indicate that only a small portion of the I-band segment of titin is elastic. We also compared passive tension developed by single rat cardiac myocytes with that of single skeletal muscle fibers and show that the strain of the titin's elastic segment is the fundamental determinant of how much passive tension cardiac muscle develops. Finally, we propose a two-stage mechanism of tension development by titin in the heart and also that titin develops an opposing force in sarcomeres that have shortened to below their slack length.

MATERIALS AND METHODS

Preparations

Myocytes

To isolate single cardiac cells we used the method of Granzier and Irving (1995). Briefly, cells were isolated from the rat (male Sprague-Dawley, ~250 g) heart by perfusing the coronary arteries with oxygenated Krebs solution containing collagenase. Atria were then removed, and the ventricles were cut into small pieces that were gently drawn several times through a plastic pipette. This released a large number of isolated cells, the majority of which had a normal, rod-like shape. Cells were then washed extensively to prevent titin from being degraded during subsequent skinning of the cells. Skinning was performed in relaxing solution with 1% Triton X-100, at 0°C for 50 min, followed by washing with relaxing solution only. To prevent titin degradation, solutions contained the protease inhibitors leupeptin and phenylmethylsulfonyl fluoride (Granzier and Irving, 1995).

Skeletal muscle fibers

Single muscle fibers were dissected from rabbit semitendinosus muscle. Adult male New Zealand White rabbits were used (weight, ~3 kg). The rabbits were anesthetized by intramuscular injection of ketamine, xylazine, and atropine (35, 7.5, and 0.02 mg/ml, respectively) and exsanguinated by removing the heart. The semitendinosus muscles were quickly removed, and each muscle was added to 40 ml of relaxing solution containing 1.0% Triton X-100. After skinning at 0°C for 50 min, the muscles were washed with relaxing solution and single fibers were dissected. Fibers were mechanically skinned and small T-shaped aluminum clips were glued to each end of the fiber. To prevent titin degradation, all solutions contained protease inhibitors. For detailed compositions of solutions and further information, see Granzier and Irving (1995).

Mechanics

Myocytes

Cells were stretched in an apparatus built on an inverted phase-contrast microscope (Nikon, model TMD). Cells were added to a temperature-controlled flow-through chamber (volume, ~150 μl), the bottom of which was a removable coverslip, which was attached to the microscope stage. A single cell was glued (glue was Great-Stuff, Insta-Foam Products, Joiliet, Illinois) at one end to a motor and at the other end to a force transducer (Model 406A, Cambridge Technology, Cambridge, MA). Additional technical information can be found in Granzier and Irving (1995). For immunolabeling experiments the cells were glued in the stretched state to the removable coverslip by first applying two small droplets of glue to the coverslip ~100 μm apart and then lowering the ends of the cell into the droplets. The cells were surrounded by a shallow ring glued to the coverslip, which served as a mini-chamber (volume, ~10 μl) for immunolabeling, fixing, and embedding of the cells (Fig. 1).

Skeletal muscle fibers

The mechanical set-up was identical to the one described above. The force transducer, however, was a strain-gauge (AME 801E, Horton, Norway). All mechanical experiments (including those on myocytes) were conducted at 20°C.

Sarcomere length measurement

Myocytes

The sarcomere length of single cardiac myocytes was measured by the method of Granzier and Irving (1995). Briefly, phase-contrast images of cells were digitized using a microcomputer and density traces along the long axis of the cell were computed. Density traces were restricted typically to a length of 50 μm and a width of 4 μm. The traces were processed by discrete Fourier transformation and the position of the first-order peak in the power spectrum was used to calculate sarcomere length. We analyzed three different regions of the cell, encompassing 50–75% of the cell width, and results from the different regions were averaged.

Skeletal muscle fibers

Sarcomere length was measured using laser diffraction. The diffraction pattern was collected with a bright-field objective and projected onto a photo-diode array. The first-order diffraction peak position was obtained, using a digital spot position detector board, and this position was converted to sarcomere length (cf. Granzier and Irving, 1995).

Protocols

In earlier passive tension work, protocols were used in which small-amplitude stretches were separated by long rest periods to allow for stress relaxation (Granzier and Wang, 1993a). However, preliminary experiments revealed that the stress disappearing during stress-relaxation is recruited back completely during the next stretch, and little is gained by the long resting periods. We therefore used a protocol in which slow continuous stretches were imposed (cf. Granzier and Irving, 1995). Myocytes and skeletal muscle fibers were stretched with a constant velocity that was chosen such that the elastic segments of titin (see Results and Discussion) were stretched by 100% in 60 s. The stretch amplitude was <~2.8 μm for cardiac cells and <~4.0 μm for skeletal muscle fibers. All curves presented in this work were highly reproducible. For a description of the data acquisition system and additional technical information, see Granzier and Irving (1995).
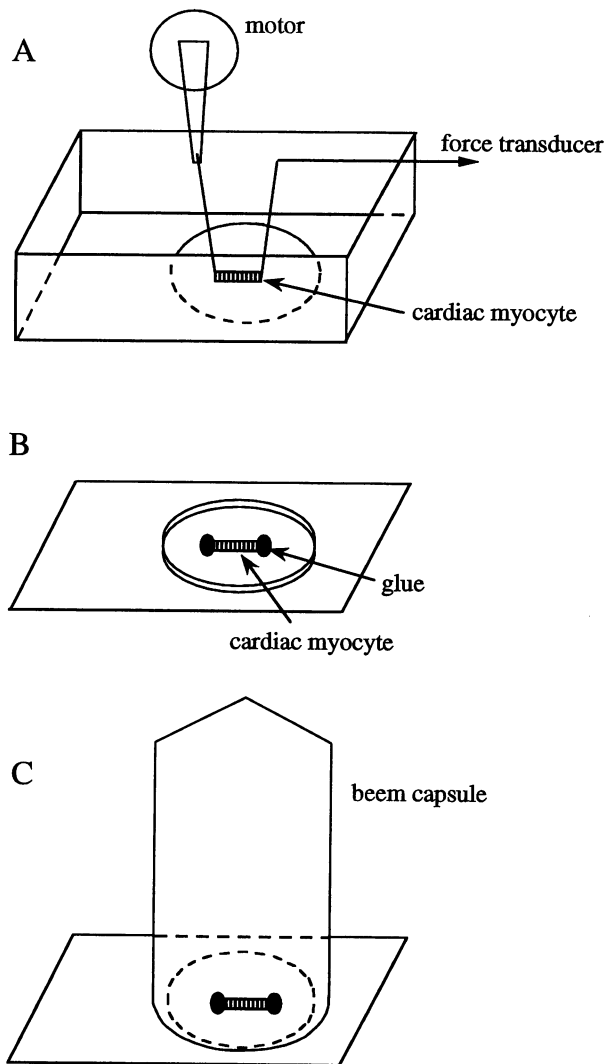
FIGURE 1 Cardiac myocyte mechanics and immunolabeling of stretched myocytes. (A) Mechanical experiments were carried out in a flow-through chamber (~150 μl) containing a removable glass coverslip as bottom. Cells were added to the small area confined by a shallow ring glued to the bottom of the chamber. A needle attached to a motor was glued to one end of the cell and another needle, attached to a force transducer, was glued to the other end of the cell. After cells were stretched, the ends of the cell were glued to the coverslip, the chamber was emptied (except for the solution in the small ring), and the coverslip was then detached from the chamber. (B) The small ring on the coverslip was used as a mini-chamber (volume, ~10 μl) for immunolabeling, fixing, and embedding of the cells. During immunolabeling the coverslip was placed in a moisture chamber at 4°C. (C) Cells were embedded by inverting a capsule filled with araldite on the coverslip, surrounding the small ring. Capsule and coverslip were then put in the oven for araldite polymerization.

Immunolabeling and electron microscopy

Cells were fixed for 20 min in freshly prepared 3% paraformaldehyde (Sigma Chemical Co., St. Louis, MO) in phosphate-buffered saline (PBS; 2.7 mM KCl; 1.5 mM KH_2PO_4; 137 mM NaCl; 8.0 mM Na_2HPO_4, 2 mM EGTA, pH 7.2). After washing the cells three times with PBS for 30 min each, cells were blocked for 30 min in PBS/0.5% bovine serum albumin (BSA; Pierce 30447H, Pierce Chemical Co., Rockford, IL). Cells were then incubated ~36 h with anti-titin monoclonal antibodies in PBS/BSA. The

following antibodies were used: T12 (2 μg/ml; Boehringer 1248–634, Boehringer Mannheim Corp., Indianapolis, IN; 9D10 (20 μg/ml; Hybridoma Bank, University of Iowa, Iowa City, IA), and Ti-102 (ascites 20X diluted). After washing cells three times (30 min each) with PBS/BSA, they were incubated for ~36 h in secondary antibody in PBS/BSA. For T12, rabbit anti-mouse IgG1 (2 mg/ml; Cappel 50227, Cappel Laboratories, West Chester, PA); for 9D10, goat anti-mouse IgG, IgA, and IgM (1 mg/ml; Cappel 55441); and for Ti-102, rabbit anti-mouse IgG whole molecule (0.2 mg/ml; Cappel 55436) was used. In several experiments the secondary antibody was nanogold Fab anti-mouse IgG (Nanoprobes 2002, diluted 20X, Nanoprobes, Inc., Stony Brook, NY). Unbound antibody was removed by washing three times for 20 min in PBS. Control cells were incubated in only secondary antibodies using the same conditions as those for the test cells. All solutions contained 100 μg/ml leupeptin and were kept at 4°C.

The anti-titin antibody T11 (Sigma T-9030) was also used. Various lots were used at concentrations between 10 and 1000 μg/ml. Several secondary antibodies were tried: rabbit anti-mouse IgG2B, nanogold Fab anti-mouse IgG (see above), and a cocktail containing all secondary antibodies used for T12, 9D10, and Ti-102. No labeling was observed. Western blot results (see below) were also negative. These findings are in contrast to the report by Fürst et al. (1988) that T11 cross-reacts with rat cardiac titin. The explanation might be a loss of immunoreactivity of T11.

Cells were fixed with glutaraldehyde/tannic acid, osmificated, and embedded in araldite (cf. Trombitás et al., 1991). The osmification step was omitted when nanogold Fab anti-mouse IgG was used and instead a silver enhancement step was introduced using HQ silver (Nanoprobes, used according to manufacturer's protocol) to increase sensitivity (K. Trombitás M. Greason, and G. Pollack, al., in preparation). The solutions needed for immunolabeling, fixing, and embedding were added while the cell remained glued to the glass coverslip inside a small 10-μl chamber (Fig. 1 B). Cells were embedded according to Trombitás and Tigyi-Sebes (1977) by inverting an araldite-filled beem capsule over the ring glued to the coverslip (Fig. 1 C). After polymerization, the coverslip was removed by using an exposure to liquid nitrogen followed by a brief exposure to ~60°C H_2O. Ultrathin sections were cut with a Sorvall MT-2 M ultramicrotome. Sections were stained with potassium permanganate and lead citrate and observed and photographed with a Hitachi H-600 electron microscope. Z-line-to-epitope distances were obtained from the electron micrographs. For spatial calibration the A-band width (1.6 μm) was used as internal standard (as in Figs. 3–5). Identical results were obtained when the microscope magnification was used for spatial calibration (see, e.g., Fig. 6).

Gel electrophoresis and Western blotting

Cells were solubilized and electrophoresed using 2–12% acrylamide gradient gels that were subsequently stained with either Coomassie blue or ammoniacal silver stain (cf. Granzier and Wang, 1993b). For Western blotting we first electrophoresed rat cardiac muscle proteins (solubilized as in Granzier and Irving, 1995) on a 2–12% gradient gel and then electrotransferred them to polyvinylidene fluoride membrane with a semidry transfer unit (Bio-Rad Laboratories, Richmond, CA) at 1.5 mA/cm² gel for 45 min using the Kyhse-Anderson buffer system (Kyhse-Anderson, 1984). The blots were boiled for 30 min in H_2O to enhance antibody sensitivity (Swerdlow et al., 1986), blocked (0.1% BSA, 0.2% gelatin, 0.1% Tween 20, and 10 U/ml heparin in PBS) for 90 min and incubated overnight at ~20°C with titin antibodies. Blots were washed with PBS/Tween 20, incubated in alkaline-phosphatase-conjugated goat anti-mouse antibody (Cappel 59294) for 2 h and then in substrate (cf. Sambrook et al., 1989) for 15 min.

Statistics

Results of our studies will be given as the mean ± SD, unless indicated otherwise. Significance values in selected parameters were examined with

the Student's t-test, and univariate linear regression was used to assess the dependence of the titin epitope locations on sarcomere length.

RESULTS

Gel electrophoresis and immunoreactivity

Solubilized rat cardiac proteins were electrophoresed on low-porosity gels, side by side with rabbit semitendinosus muscle (Fig. 2 A). Cardiac titin consisted of a doublet, T_1 and T_2 (Fig. 2 A). T_2 is generally considered a product of degradation of the parent molecule, T_1, a process occurring during sample preparation (Wang, 1985). The degree of degradation in rat cardiac samples is typical of the degradation seen in most skeletal muscles, with the exception of rabbit semitendinosus muscle, which is known to be relatively insensitive to degradation (Wang et al., 1991). T_1 of rat cardiac muscle migrated much further on the gels than T_1 of skeletal muscle (Fig. 2 A), confirming the earlier finding that rat cardiac muscle expresses a low molecular mass size variant of titin (Granzier and Irving, 1995).

The immunoreactivities of the antibodies used in this study (T12, 9D10, and Ti-102) were tested by Western blotting of rat heart muscle proteins. All three antibodies were specific for titin (Fig. 2 B), as expected from the work by others (Wang and Greaser, 1985; Fürst et al., 1988; Jin, 1995). T12 and 9D10 reacted only with the titin T_1 band (Fig. 2 B), whereas the Ti-102 antibody reacted with both T_1 and T_2 (Fig. 2 B).

Immunolabeling of stretched myocytes

Excellent results were obtained with our method of immunolabeling of stretched single myocytes (Fig. 1). Because the ends of the cells were glued to the coverslip on top of which an araldite-filled beem capsule was placed for embedding, cells were not only ideally oriented for sectioning, they were also so close to the surface of the araldite block that they could be found with relative ease. Of the more than 60 stretched cells that we mounted, not a single cell was lost during subsequent processing.

The structure of myocytes was well preserved. In control sarcomeres labeled with only secondary antibody, the usual structural features could be observed (Fig. 3 A). There was

FIGURE 3 Sarcomere location of T12 titin epitope. (A) High magnification image of control sarcomeres (not labeled). The arrow indicates a faint line that can be seen in the I-band. (B) High magnification micrographs of sarcomeres labeled with T12 primary antibody and with secondary antibody. The upper panel shows a micrograph from a short sarcomere and the bottom panel a micrograph from a long sarcomere. In both sarcomeres, dense stripes on both sides of the Z-line can be seen (arrows). (C) Sarcomere labeled with T12 and with a nanogold-conjugated secondary antibody that was silver enhanced. Because the cell was not osmificated, less structural detail can be seen than in A and B. Note the dark stripes (arrows) close to the Z-lines. Scale bars denote 1 μm. (D) sarcomere length dependence of distance between the T12 epitope and the center of the Z-line. The linear regression line fitted to the data is shown. See text for further details.
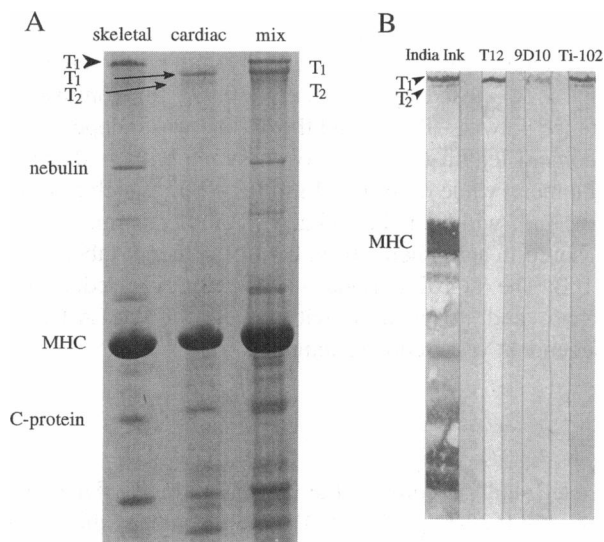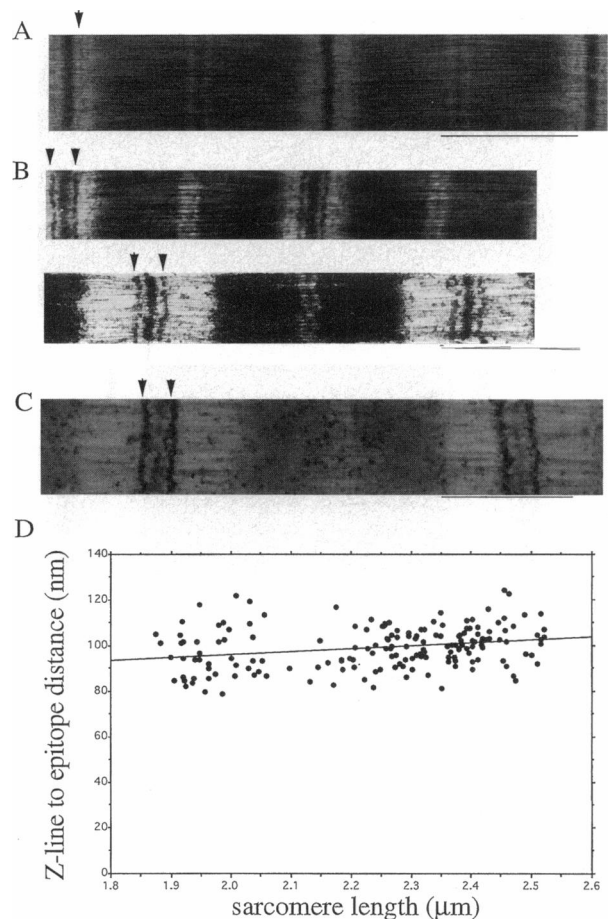
FIGURE 2 (A) Sodium dodecyl sulfate polyacrylamide gel electrophoresis of rat cardiac and rabbit skeletal muscle (semitendinosus). Cardiac titin consists of a doublet, T_1 and T_2. T_1 of cardiac muscle (lane 2) migrates much further into the gel than skeletal muscle titin (lane 1), which is especially evident when cardiac and skeletal muscle titin are mixed (lane 3). (B) Immunoreactivity of cardiac titin. T12 and 9D10 react with only T_1, whereas Ti-102 reacts with both T_1 and T_2. The same result with T12 has been reported by Fürst et al. (1988) using chicken cardiac muscle proteins.

sometimes a faint line close to the Z-line, which may correspond to the N_1-line described in skeletal muscle (Franzini-Armstrong, 1970). Excellent antibody penetration was obtained as evidenced by uniform immunolabeling throughout the cross-section of the cell (e.g., Fig. 4 A). Results obtained with the different anti-titin antibodies (T12, 9D10, and Ti-102) are detailed below.

T12

When cardiac cells were labeled with the anti-titin antibody T12, a single stripe appeared in the I-band of each half-sarcomere, approximately 100 nm from the Z-line (Fig. 3
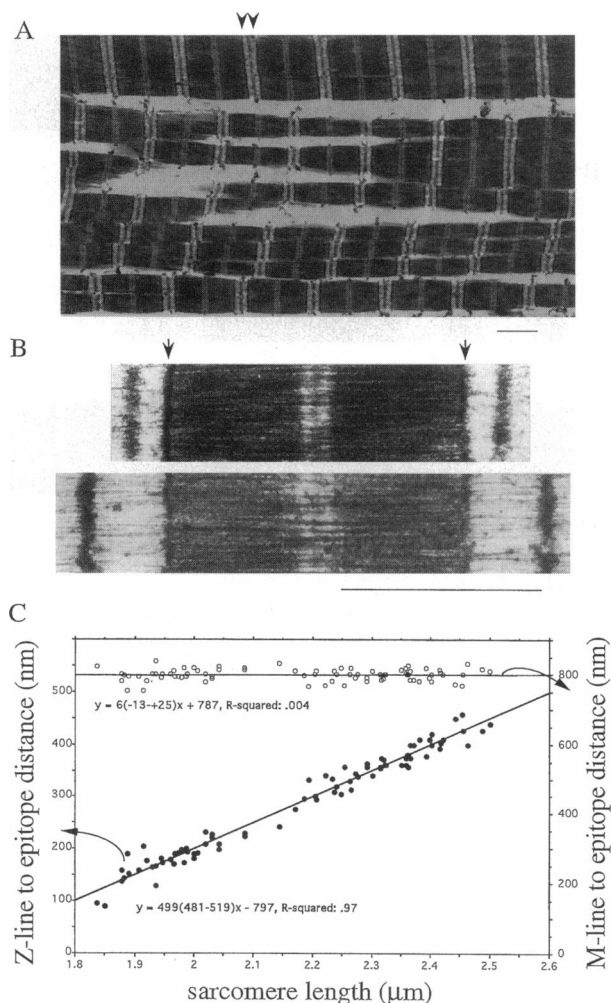

FIGURE 4 Sarcomere location of Ti-102 epitope. (A) Low magnification micrograph of single cardiac myocyte labeled with Ti-102. Average sarcomere length is ~2.0 μm. Ti-102 labels the ends of the A-bands (see *arrowheads*). Note that immunolabeling occurred uniformly in all sarcomeres. (B) High magnification micrographs of sarcomeres labeled with Ti-102. The upper panel shows a micrograph from a short sarcomere and the bottom panel a micrograph from a long sarcomere. In both cases, only the ends of the A-band are labeled (see *arrows*). Scale bars, 1 μm. (C) sarcomere length dependence of Ti-102 epitope position in the sarcomere. The indicated linear regression equations show in parentheses the 95% confidence interval of the slopes. See text for details.

B). Because this stripe is in a position similar to that of the N_1-line in control sarcomeres (Fig. 3 A), we tested whether it was indeed a result of additional protein densities of bound T12 and the secondary antibody, or that it was simply the N_1-line. Cells were therefore first labeled with T12 and then with gold-conjugated Fab fragments as secondary antibody, followed by silver enhancement of the gold beads. This revealed intense dark silver-based stripes close to the Z-line (Fig. 3 C) in a position similar to the one found when protein-based densities were used (Fig. 3 B), indicating that the latter did indeed report the location of the titin epitope to which T12 binds.

The location of the T12 epitope in the sarcomere was studied as a function of sarcomere length by measuring the distance between the center of the Z-line and the center of the T12 epitope (Fig. 3 D). There was a tendency for the T12 epitope to move slightly away from the center of the Z-line when the sarcomere length was increased (Fig. 3 D). Linear regression analysis showed that the correlation coefficient between sarcomere length and Z-line-to-epitope distance was low ($r = 0.26$) and that the overall increase in epitope distance was relatively small (Fig. 3 D). Therefore we assumed that, over the studied sarcomere length range (~1.8–2.5 mm), the distance between the T12 epitope and the Z-line is independent of sarcomere length. This is consistent with the findings of studies on skeletal muscle by Fürst et al. (1988) and Trombitás and Pollack (1993).

Ti-102

In each half-sarcomere the Ti-102 antibody labeled a single epitope at the edge of the A-band, both in short and long sarcomeres (Fig. 4, A and B). The distance between the Z-line and this epitope varied linearly with sarcomere length (Fig. 4 C, closed symbols; $r = 0.99$). In contrast, the distance between Ti-102 and the M-line was independent of sarcomere length (Fig. 4 C, open symbols; $r = 0.06$) and had a mean value of 799 ± 4 nm ($n = 80$), which is similar to the half-width of the A-band (810 ± 15 nm; $n = 63$) measured in sarcomeres from control cells not labeled with Ti-102. The Ti-102 epitope is thus at the very edge of the A-band, and its position with respect to the A-band is independent of sarcomere length.

9D10

In each half-sarcomere the 9D10 antibody labeled an epitope in the I-band (Fig. 5 A). The location of this epitope was approximately in the middle of the segment demarcated by T12 and Ti-102, as revealed by cells that had been triple labeled with 9D10, T12, and Ti-102 (Fig. 5 B). Notably, when cells were labeled very strongly (by increasing the concentration of the primary antibody), the 9D10 stripe appeared to broaden asymmetrically by widening preferentially toward the M-line (results not shown). To prevent this phenomenon from affecting our results, the position of the
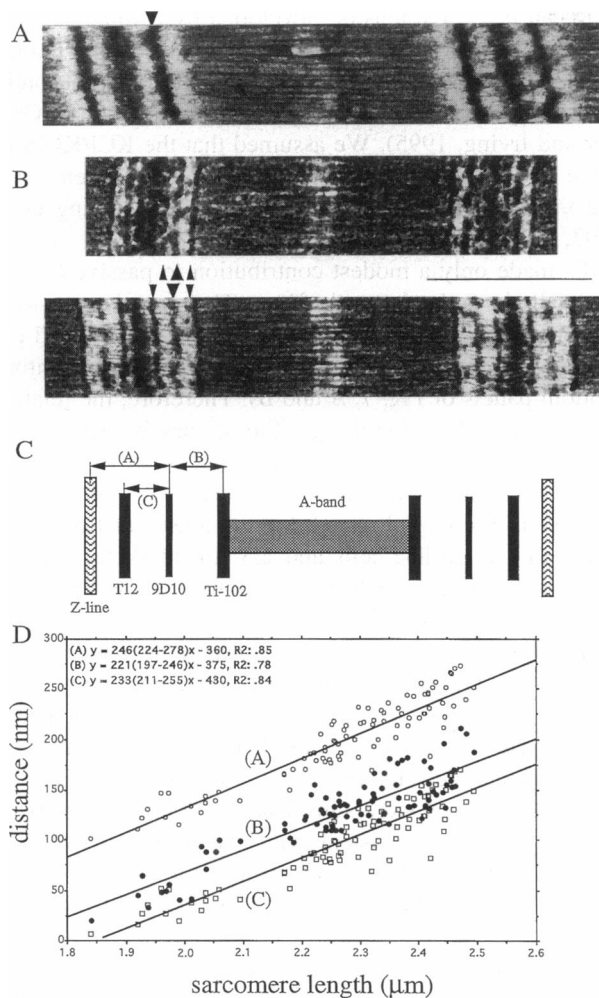
FIGURE 5 Sarcomere location of 9D10 epitope. (A) Sarcomere labeled with 9D10, revealing a darkly stained stripe in the I-band (see *arrow*). (B) Sarcomeres that had been triple labeled with T12, 9D10, and Ti-102. The upper panel shows a micrograph from a short sarcomere and the bottom panel a micrograph from a long sarcomere. In both panels the 9D10 epitope (*large arrowhead*) is approximately in the middle between the T12 (*left small arrowhead*) and Ti-102 (*right small arrowhead*) epitopes. Scale bars, 1 μm. (C) Schematic representation of the segments demarcated by the Z-line and the various titin epitopes. (D) Sarcomere length dependence of titin segments demarcated by the Z-line and 9D10 (segment A), 9D10 and Ti-102 (segment B), and T12 and Ti-102 (segment C). The lengths of each of the three segments varied linearly with sarcomere length. The linear regression lines had similar slopes but were vertically displaced. The indicated linear regression equations show in parentheses the 95% confidence interval of the slopes.

9D10 epitope was analyzed only in sarcomeres that were labeled as in Fig. 5.

We measured the lengths of the sarcomeric segments between the Z-line and the 9D10 epitope and between the 9D10 and Ti-102 epitopes (segments A and B, respectively, in Fig. 5 C). Results are shown in Fig. 5 D. The lengths of both segments increased linearly with increasing sarcomere length ($r \approx 0.9$). The regression lines of the two segments had similar slopes (95% confidence intervals, 225–278 nm/μm for A and 211–255 nm/μm for B), indicating that,

for a given degree of sarcomere stretch, the 9D10 epitope moved away from both the Z-line and the A-band by a similar distance. Thus, segments A and B have similar overall elasticity.

Although the overall elasticities of segments A and B are similar, both segments might contain inelastic segments. Segment A contains an ~100-nm titin segment between the Z-line and T12, which is inelastic (see above). The presence of this inelastic segment is not expected to affect the slope of the regression line A; rather, it merely displaces this line vertically. Indeed, the linear regression line obtained for the T12-to-9D10 distance (segment C in Fig. 5) had a slope similar to that of A but was shifted down by ~100 nm (Fig. 5 D). Furthermore, segment C reached a length of zero at a sarcomere length of ~1.85 μm, indicating that it is likely that segment C is fully elastic and does not contain inelastic segments. As for segment B, the slope of its linear regression line is similar to that of segment C, but the line is vertically shifted upwards by ~25 nm (Fig. 5 D), indicating that segment B may contain an ~25-nm inelastic region. This is consistent with the study of Trombitás et al. (1991) that revealed that, in skeletal muscle, a narrow I-band region adjoining the A-band is inelastic.

In summary, the elastic segment of rat cardiac titin is much shorter than the entire I-band segment. Previously we estimated the contour length of the total I-band segment of unstrained titin to be ~200 nm (Granzier and Irving, 1995). Based on the above data it is likely that the ~100-nm titin segment next to the Z-line and the ~25-nm segment close to the A-band are inextensible over the physiological sarcomere length range (~1.8–2.4 μm; Rodriguez et al., 1992). This leaves ~75 nm as the length of titin's elastic I-band segment that is able to develop passive tension when strained.

Immunolabeling of shortened cells

We also studied cells that were unattached during labeling, many of which were at the slack length (~1.85 μm), whereas some had shortened before fixation. In short sarcomeres the T12 epitope was still found some distance from the Z-line (Fig. 6). At a sarcomere length of ~1.3 μm, the T12 epitope was 89 nm away from the Z-line, down from an average of 95 nm in sarcomeres of 1.85 μm in length. As for the 9D10 and Ti-102 epitopes, only moderately shortened sarcomeres were investigated. At such lengths these epitopes merged with the T12 epitope and could not be discerned as separate (Fig. 6), indicating that the end-to-end length of the elastic titin segment was negligible.

Passive tension

It is known from earlier work (Granzier and Irving, 1995) that the increase of passive tension of cardiac cells is much steeper than that of skeletal muscle fibers when plotted as a function of sarcomere strain. This difference is much
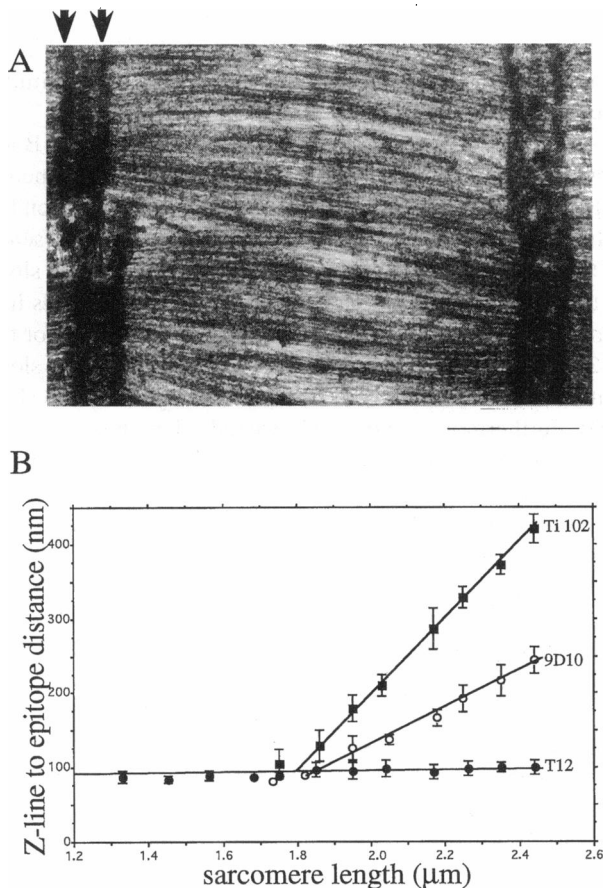
FIGURE 6 Titin behavior in short sarcomeres. (A) Short sarcomere (~1.7 μm) labeled with T12, 9D10, and Ti-102. No separate epitopes can be seen. Instead, a single dark stripe is present in each I-band (arrows), approximately 100 nm from the center of the Z-line. Scale bar, 0.5 μm. (B) Sarcomere length dependence of distance between the Z-line and T12 (●), the Z-line and 9D10 (○), and the Z-line and Ti-102 (■). Epitopes converge at a sarcomere length of ~1.8 μm. See text for further details. For clarity's sake, results were grouped in sarcomere length bins of 0.1 μm. Mean values ± SDs are shown for distances. For sarcomere length, the mean value of all data in the bin is given. (Note that thick filaments in A are slightly bent, despite that the sarcomere is longer than the A-band width. Bending may result from a compressive force exerted by titin when sarcomeres shorten below the slack length. See Discussion and Fig. 9.)

smaller when passive tension is plotted against the strain of the total titin I-band segment. Our immunolabeling experiments revealed that the elastic portion of cardiac titin is much shorter than the I-band segment. Therefore we analyzed how passive tension varies with (1) sarcomere strain, (2) strain of the total I-band segment of titin, and (3) strain of the extensible segment of titin. Rat cardiac cells and single fibers from rabbit semitendinosus muscle were used for comparing the two muscle types. We chose the semitendinosus muscle because it expresses the largest titin size variant known in mammalian muscle (Wang et al., 1991, 1993), making it ideal for a comparison because its titin is as different from cardiac titin as possible. The lengths of the total I-band segments and elastic segments of cardiac and skeletal muscle titins that were assumed are shown in Table

1. Because passive tension developed by cardiac cells and skeletal muscle fibers is derived not only from titin but also from intermediate filaments, we dissected the contribution of titin to passive tension using KCl/KI treatment (cf. Granzier and Irving, 1995). We assumed that the KCl/KI-insensitive tension is derived from intermediate filaments (IFs) and the KCl/KI-sensitive tension from titin (Wang et al., 1993; Granzier and Irving, 1995).

IFs made only a modest contribution to passive tension, especially in skeletal muscle fibers. Thus, passive tension is predominantly derived from titin (Fig. 7). Titin-based passive tension increased with sarcomere length exponentially (bottom panels of Fig. 7, A and B). Therefore, the relationship between the natural logarithm of passive tension and sarcomere length is linear (top panels of Fig. 7, A and B). The linear relationship started only at lengths slightly longer than slack. We hypothesized that the linear relation started at 2.0 μm in cardiac cells and 2.3 μm in skeletal muscle fibers because this is where titin elongation is expected to start (see Discussion). To test this hypothesis, results from cardiac cells below and above 2.0 μm were fitted by separate lines, and the significance of the difference between the slopes of the lines was determined. An identical procedure was carried out for skeletal muscle results below and above 2.3 μm. Examples are shown in the top panels of Fig. 7, A and B. The slopes were significantly different ($p = 0.05$). Results are thus consistent with the hypothesis that the exponential passive tension rise starts at a sarcomere length of ~2.0 μm in cardiac cells and ~2.3 μm in skeletal muscle fibers.

Results from all experiments were averaged and passive tension was plotted against sarcomere strain, the strain of the I-band segment of titin, and the strain of the elastic segment of titin. Fig. 8 A shows that passive tension of cardiac myocytes increased much steeper with sarcomere strain then that of skeletal muscle fibers. The difference decreased when passive tension was plotted against the strain of the I-band segment of titin (Fig. 8 B), and the difference became negligible when passive tension was plotted against the strain of the elastic segment of titin (Fig. 8 C). The exponent of the exponential tension rise was also determined for passive tension versus sarcomere strain, I-band segment strain, and elastic segment strain (Table 1). At the sarcomere strain and I-band segment strain level, results of cardiac cells and skeletal muscle fibers were significantly different ($p = 0.001$ and 0.02), whereas at the elastic segment level, results were essentially identical ($p = 0.94$).

The results presented above were based on the molecular masses and lengths of skeletal and cardiac titins shown in Table 1. We also studied how the conclusions from our study would differ if the length of rabbit semitendinosus titin were to be 1.25 μm, as determined for rabbit back muscle by Suzuki et al. (1994) and the length of cardiac titin were to be 1.03 μm (determined by estimating its molecular mass as in Granzier and Irving, 1995, and using as high molecular weight standards rabbit back muscle T1 and T2

TABLE 1   Titin and passive tension

	Rat cardiac myocytes ($n = 7$)	Rabbit semitendinosus muscle ($n = 5$)	p value
Titin			
M_r (MDa)	2.49*	2.94[‡]	
Contour length of unstrained titin (μm)			
In the A-band	~800*	~800[‡]	
In the I-band	~200*	~350[‡]	
Inelastic I-band segment	~125 (this study)	~150[§]	
Elastic I-band segment	~75 (this study)	~200[§]	
Slack sarcomeres			
Length (μm)	1.86 ± 0.04	2.06 ± 0.02	
End-to-end length of elastic titin segment (μm)	0.005	0.08	
Strain of elastic titin segment[¶]	0.07	0.4	
Exponent of exponential tension rise[‖]			
Tension vs. sarcomere strain	14.3 ± 3.9	5.9 ± 0.5	0.001
Tension vs. I-band segment strain	3.1 ± 0.9	2.0 ± 0.2	0.02
Tension vs. elastic titin segment strain	1.15 ± 0.30	1.14 ± 0.01	0.94

*From Granzier & Irving (1995).
[‡]From Wang et al. (1991).
[§]Based on findings by Trombitás et al. (1991) and Trombitás & Pollack (1993).
[¶]Strain (ϵ) defined as L/L_0. L_0 is the contour length of the unstrained elastic titin segment. Strains between 0.0 and 1.0 indicate that the elastic titin segment is folded onto itself (as in Fig. 9 A). The elastic titin segment has a strain of 0.0 in sarcomeres with a length that equals the A-band width plus twice the contour length of the inelastic I-band segment of titin. This corresponds to 1.85 μm for cardiac muscle and 1.90 μm for skeletal muscle.
[‖]Slope of natural logarithm of titin-based passive tension versus strain. Strains were calculated over a sarcomere length range of 2.0–2.35 μm for cardiac cells and 2.3–3.0 μm for skeletal muscle fibers.

with the same molecular masses and linear masses given in Suzuki et al., 1994). The passive tension versus titin's I-band segment strain curve and the passive tension versus the elastic titin segment strain curve of both cardiac and skeletal muscle (results not shown) were slightly different from those in Fig. 8, B and C. However, unchanged was our conclusion that, at the sarcomere strain and I-band segment strain level, results of cardiac cells and skeletal muscle fibers were significantly different, whereas at the elastic segment level, results were essentially identical.

DISCUSSION

We studied titin in cardiac muscle and explored the size of titin's I-band segment that is elastic and involved in the development of passive tension. Specific locations along the titin molecule were marked by monoclonal antibodies, and their positions were followed by immunoelectron microscopy, after stretching the sarcomere to varying lengths. Only a small fraction of the I-band segment of titin turned out to be elastic. Passive tension measurements of both single cardiac myocytes and single skeletal muscle fibers showed that the fundamental determinant of how much passive tension a striated muscle develops is the strain of the elastic I-band segment of titin. Our findings led us to propose a model in which titin develops tension not only when sarcomeres are stretched beyond their slack length (passive tension) but also when they shorten to lengths below slack (opposing force).

Antibodies

Titin consists of a long string of repeating sequence motifs with a high degree of sequence homology (Labeit et al., 1990, 1992; Maruyama at al., 1993; Fritz et al., 1993; Pan et al., 1994), and depending on the experimental conditions of immunolabeling, some anti-titin antibodies may bind to more than one epitope. Thus, the results found in this study apply to the epitopes bound most strongly by the antibodies under the experimental conditions that were used. The antibody T12 was raised against the T_2 component of skeletal muscle titin and has been shown to cross-react with rat cardiac titin by immunofluorescence of frozen tissue sections (Fürst et al., 1988). Our work confirms this cross-reactivity (Fig. 2 B). The antibody 9D10 was raised against bovine cardiac titin (Wang and Greaser, 1985) and Ti-102 against a genetically expressed rat cardiac titin fragment that contains a single class II sequence motif (Jin, 1995). Both antibodies have been used for immunofluorescence studies on cardiac myofibrils, and these studies revealed that both 9D10 and Ti-102 label a broad region in the I-band close to the A/I junction (Wang and Greaser, 1985; Jin, 1995). The present electron microscopic study is in general agreement with these results and because of its higher resolution further extends these findings.

We found in Western blots of rat cardiac muscle proteins that T12 and 9D10 react only with T_1, whereas Ti-102 reacts with both T_1 and T_2 (Fig. 2 B). These findings indicate that the T12 and 9D10 epitopes are on the small segment (difference segment) of the titin molecule, which is cleaved away from T_1 during its degradation into T_2, in
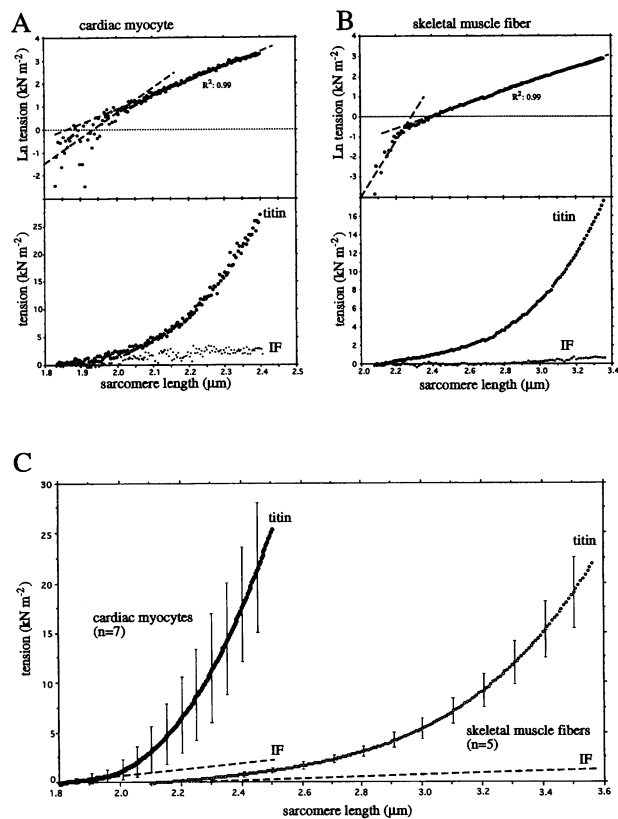
FIGURE 7 Passive tension-sarcomere length relations of rat cardiac myocytes and rabbit skeletal muscle fibers (semitendinosus). (A and B, bottom panels) Sarcomere length dependence of KCl/KI-sensitive tension (titin) and KCl/KI-insensitive tension (IFs). Titin-based tension is much larger than IF-based tension. (A and B, top panels) Natural logarithm of titin-based tension versus sarcomere length. Results of cardiac myocytes at lengths <2.0 μm and those at lengths >2.0 μm were fitted by two straight lines. The 95% confidence intervals of the slopes of these lines were 7.1–14.7 and 6.2–6.5, respectively. Results of skeletal muscle fibers at lengths <2.3 μm and at >2.3 μm were also fitted by two separate straight lines, and their 95% confidence slope intervals were 10.8–16.6 and 3.0–3.1, respectively. (C) Comparison of titin-based and IF-based tensions from cardiac myocytes and skeletal muscle fibers. Results of seven myocytes and five skeletal muscle fibers were pooled, and their mean values and SDs are shown (for clarity's sake the SD is displayed for only some of the data points, whereas for IFs only a linear fit to the data is shown.) At a given sarcomere length, cardiac titin developed much higher passive tensions than skeletal muscle fibers did.
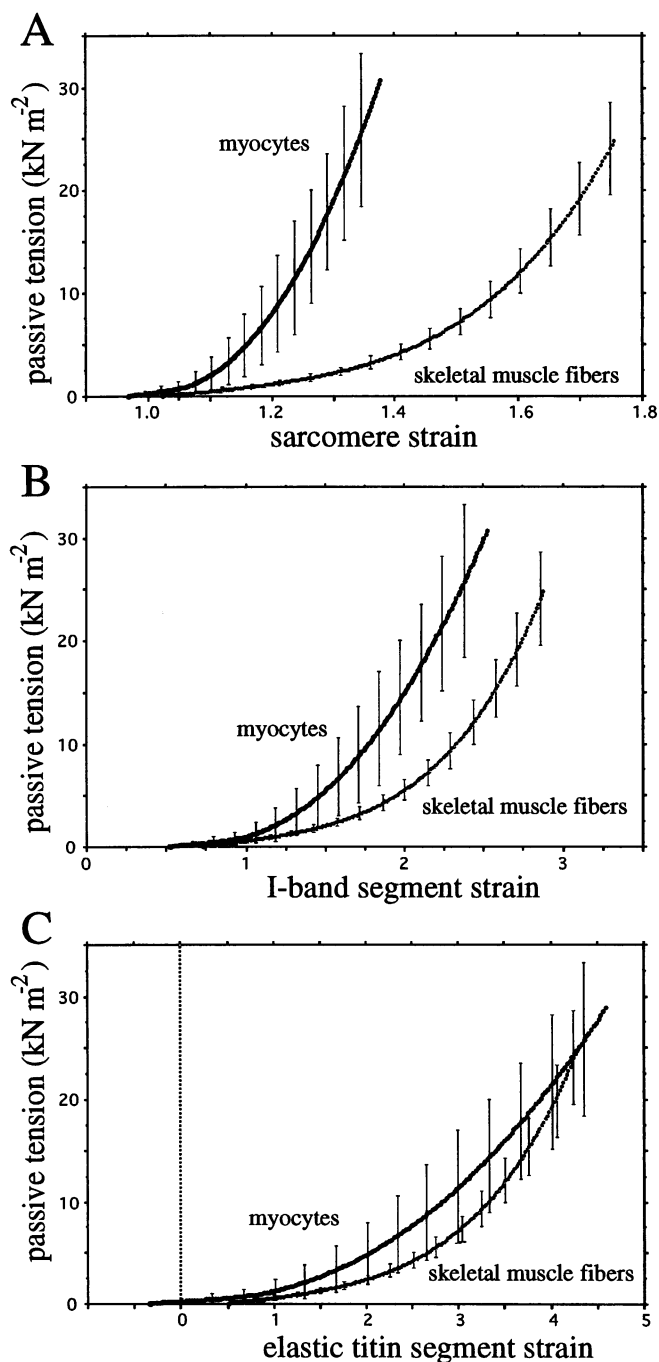
FIGURE 8 Dependence of titin-based passive tension on (A) sarcomere strain, (B) strain of total I-band segment of titin, and (C) strain of the elastic I-band segment of titin. Strain defined as L/L0. See Table 1 and text for further information. (Mean ± SDs are shown. For clarity's sake the SD is displayed for only some of the data points. Same data as in Fig. 7 C.)

contrast to Ti-102. Because T12 and 9D10 label in the I-band (Figs. 3 and 5), the difference segment of cardiac titin is part of the I-band segment of titin but does not extend to the A/I junction where the Ti-102 epitope is found (Fig. 4). These findings are in agreement with the location of the difference segment of titin in skeletal muscle (Itoh et al., 1988; Fürst et al., 1988; Maruyama et al., 1993).

Inelastic titin segment

In skeletal muscle a single titin molecule spans from the Z-line to the M-line (Itoh et al., 1988; Fürst et al., 1988).

The full extent of the titin molecule in the cardiac sarcomere has not been established yet. It is likely that in rat cardiac myocytes a single titin molecule extends beyond the T12 epitope toward the Z-line and beyond the Ti-102 epitope toward the M-line. This is based on biochemical studies in which it was found that rat cardiac titin cross-reacts with titin antibodies that in skeletal muscle label either between

the M-line and the edge of the A-band or in the region between the middle of the Z-line and the T12 epitope (Fürst et al., 1988). Furthermore, in recent immunolabeling studies repetitive titin epitopes were found in the A-band of cardiac muscle (Trombitás, unpublished observations). Thus, it is likely that in cardiac muscle a single titin molecule spans from the Z-line to the M-line, as it does in skeletal muscle.

Over the sarcomere length range studied ($\sim$1.8–2.5 μm) the T12 epitope maintains a fixed position relative to the Z-line (Fig. 3), whereas the Ti-102 epitope is stationary with respect to the M-line (Fig. 4). The titin segment between the Z-line and T12 epitope and the segment between the Ti-102 epitope and the M-line are thus inelastic. However, these segments are intrinsically elastic, because we recently found that, after thin filament removal with gelsolin and thick filament extraction with high ionic strength relaxing solution, both the T12 and Ti-102 epitopes translocated toward the center of the I-band when sarcomeres were stretched (Trombitás and Granzier, in preparation). It is thus likely that under physiological conditions the Z-line-to-T12 titin segment and the Ti-102-to-M-line segment are rendered inelastic by their association with thin filament and thick filament proteins, respectively.

Earlier we estimated the contour length of unstretched rat cardiac titin to be $\sim$1.0 μm (Granzier and Irving, 1995). Our present findings indicate that the $\sim$0.8-μm titin segment that is attached in the A-band and the $\sim$0.1-μm segment that is attached in the I-band between the Z-line and T12 epitope are inelastic. This leaves $\sim$0.1 μm of the titin molecule to span from the T12 to Ti-102 epitopes.

Elastic titin segment

The sarcomere length dependence of the 9D10 epitope position, relative to that of the T12 and Ti-102 epitopes, allows us to estimate how much of the $\sim$0.1-μm titin segment between T12 and Ti-102 is elastic. Because the distance between the 9D10 and T12 epitopes approaches zero in sarcomeres that are slack (segment C in Fig. 5 D), it is likely that the titin segment between 9D10 and T12 is completely elastic and does not contain inelastic segments. On the other hand, the length of the segment between the 9D10 and Ti-102 epitopes (segment B in Fig. 5 D) does not approach zero in slack sarcomeres; its length-to-sarcomere-length relationship has a slope similar to that of segment C but is displaced vertically by $\sim$25 nm (Fig. 5 D). This indicates that the titin segment between 9D10 and Ti-102 is not entirely elastic but contains an $\sim$25-nm inelastic segment. It is not clear why this region is inelastic. Titin could be intrinsically inelastic in this region or it may be rendered inelastic because of its interaction with other structures in the sarcomere, for example, with the tapered ends of the thick filaments. Our results are similar to those from mammalian skeletal muscle, where the I-band segment of titin has been shown to contain a 50-nm inelastic segment close to the A/I junction (Fürst et al., 1988; Trombitás et al.,

1991). The finding that the inelastic segment is shorter in cardiac muscle than in skeletal muscle (25 nm vs. 50 nm) suggests that part of the skeletal muscle titin molecule is not expressed in cardiac muscle. This possibility is supported by several titin antibodies that have been described that in skeletal muscle label the I-band segment of titin in close proximity to the A/I junction (Fürst et al., 1988) but that do not cross-react with rat cardiac titin (Hill and Weber, 1986). The presence of an $\sim$25-nm inelastic titin segment in cardiac muscle between the T12 and Ti-102 epitopes leaves only an $\sim$75-nm segment with elastic properties.

Cardiac titin versus skeletal muscle titin

Most skeletal muscles express much larger size variants of titin than cardiac muscle does (Hu et al., 1986; Wang et al., 1991; Granzier and Irving, 1995). Although it is difficult to be certain about the exact molecular mass and length of titin (Maruyama, 1994; Suzuki et al., 1994), we will assume that the skeletal muscle used in this study (rabbit semitendinosus muscle) contains titin with a molecular mass of 2.94 MDa and an end-to-end length of 1.15 μm, of which 0.8 μm is found in the A-band and 0.35 μm in the I-band region of the sarcomere (Wang et al., 1991). As we found for cardiac muscle, the T12 epitope is located in skeletal muscle 0.1 μm away from the center of the Z-line and does not translocate when sarcomere length is changed (Fürst et al., 1988; Trombitás and Pollack, 1993). As discussed above, the I-band of skeletal muscle also contains a 50-nm inelastic segment adjoining the A/I junction (Fürst et al., 1988; Trombitás et al., 1991; Trombitás and Pollack, 1993). This leaves in rabbit semitendinosus muscle $\sim$0.2 μm as the length of the elastic titin segment. Thus, in this muscle type, the total length of the titin molecule is $\sim$15% longer than that of cardiac muscle (1.15 μm vs. 1.0 μm), but the elastic titin segment is $\sim$170% longer (0.2 μm vs. 0.075 μm).

The elastic titin segment and passive tension

Titin-based passive tension increases much more steeply with sarcomere strain in cardiac myocytes than in skeletal muscle fibers (Figs. 7 and 8). Results from these two muscle types are much more similar when passive tension is expressed as a function of the strain of the total I-band segment of titin (Fig. 8 B), confirming earlier results (Granzier and Irving, 1995). Because of our new finding that part of the I-band segment is inelastic, we included in the present study a passive tension comparison at the level of the elastic I-band segment of titin. Results from cardiac and skeletal muscles were statistically indistinguishable (Fig. 8 C; Table 1).

An important consideration in comparing titin-based passive tension from skeletal and cardiac muscle is whether or not the number of titin filaments per unit cross-sectional area is the same in the two muscle types. The number of titin filaments can be calculated from the number of thick fila-
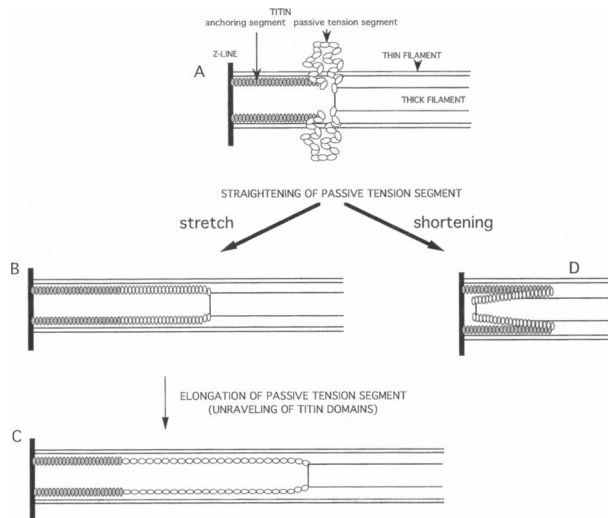
FIGURE 9 Working hypothesis of molecular mechanism of passive tension generation by titin in cardiac muscle. The I-band segment of titin consists of two subsegments: an inelastic anchoring segment and an elastic passive tension segment. The ~100-nm-long anchoring segment is attached to the Z-line and runs parallel to the thin filament, whereas the elastic segment connects the anchoring segment to the thick filament. The anchoring segment does not change length when the sarcomere length is altered. The elastic segment is in slack sarcomeres not straight, but highly folded (A), whereas upon sarcomere stretch this segment first straightens (A and B) and then elongates by unraveling (B and C), developing passive tension in the process. In this model, straightening of the passive tension segment also occurs when sarcomeres shorten to below their slack length (D). See text for further details. The short inextensible I-band segment of titin in close proximity to the A-band and the titin segment in the A-band region of the sarcomere are ignored in this schematic for clarity's sake. Furthermore, it is likely that in reality more than two titin filaments connect to one end of the thick filament and that close to the Z-line titin filaments form a lateral network (Funatsu et al., 1993).

ments per unit cross-sectional area and the number of titin filaments per thick filament. Previously, we showed that the number of thick filaments per unit cross-sectional area of cardiac muscle is similar to that of rabbit semitendinosus muscle (see Discussion of Granzier and Irving, 1995). As for the number of titin filaments per thick filament, it has typically been estimated at approximately 6 titin molecules per half-thick-filament in both skeletal and cardiac muscle (Wang, 1985; Maruyama, 1986; Trinick, 1991; Granzier and Irving, 1995). A recent study suggests, however, an average of 4.5 titin molecules per half-thick-filament in rabbit skeletal muscle and only 3 titin molecules per half-thick-filament in rabbit cardiac muscle (Suzuki et al., 1993). A consequence of such differences would be that the similar passive tension-elastic titin segment strain curves of cardiac and skeletal muscle (Fig. 8 C) would become different at the single titin molecule level. In contrast to passive tension, the exponent of the exponential passive tension rise (Fig. 7, A and B) is independent of the number of titin filaments per unit cross-sectional area of the preparation. Thus it is a good additional measure for comparison of cardiac and skeletal muscle titins. Although the exponents of cardiac and skeletal muscle

are quite different at both the sarcomere strain and I-band strain level, results of cardiac and skeletal muscle are essentially identical when passive tension is expressed as a function of the strain of the elastic titin segment (Table 1). Thus, the elastic titin segment is the fundamental determinant of how steeply passive tension increases with strain.

An effective means of manipulating passive tension is by varying the length of the extensible titin segment, and this is likely to underlie the existence of the titin size variants found in different muscles (Hu et al., 1986; Wang et al., 1991; Horowits, 1992). As for cardiac muscle, titin is ~15% smaller than rabbit semitendinosus muscle, but at the level of the elastic titin segment this modest difference is amplified to 170%, allowing cardiac muscle to develop high levels of passive tension for a modest degree of sarcomere extension (Fig. 7 C).

Mechanism of passive tension development

We propose that passive tension is developed by both straightening of the elastic segment of titin and by unraveling of the different domains that make up this segment. As for straightening, in cardiac sarcomeres that are ~1.85 μm long the T12, 9D10, and Ti-102 epitopes all merge together (Fig. 6), indicating that at this length the elastic titin segment is highly folded. This highly folded state is probably similar to that of the nodules that are often seen when purified native titin is viewed in the electron microscope in the absence of special orientation techniques (Maruyama et al., 1984; Wang et al., 1984b; Trinick et al., 1984) and to that of the highly retracted titin seen in sarcomeres that have been "freeze-broken" (Trombitás et al., 1993). The entropy of such a highly folded titin segment is high, and force needs to be exerted to straighten the segment and lower its entropy (Florey, 1969; Higuchi et al., 1993). In cardiac muscle, this force will be maximal at a sarcomere length of ~2.0 μm because that is where the elastic titin segment will be completely straight. Using the measured passive tension of cardiac myocytes at a sarcomere length of 2.0 μm (Fig. 7) we estimated that the force required for complete straightening of the elastic segment of a single titin molecule is ~1 pN, which is similar to the values estimated from light-scatter studies of isolated titin in solution (Higuchi et al. 1993). It is also noteworthy that it is likely that, in the A-band, the titin molecule is straight because of its binding to the thick filament and that upon thick filament extraction titin will tend to fold and exert a force that can shorten the sarcomere. This may explain the finding by Roos and Brady (1989) and Higuchi et al. (1992) that after thick filament extraction the slack sarcomere length decreases.

When the elastic titin segment is completely straight, further sarcomere stretch will elongate the elastic segment of titin. The molecular organization of titin has been shown by cDNA cloning and sequencing to be modular. Two classes of ~100-residue domains, type I and type II, repeat along the molecule (Labeit et al., 1990, 1992; Fritz et al., 1993; Pan et al., 1994),

and the I-band portion of titin contains long stretches of exclusively type II domains (Maruyama, 1994; Sebestyén et al., 1995). It is thus likely that the elastic titin segment elongates by unraveling of the polypeptides that make up the type II domains (Erickson, 1994). Our mechanical study showed that such unraveling results in passive tension increasing exponentially with sarcomere length, as has been shown by others (Wang et al., 1991, 1993; Granzier and Wang, 1993c). Furthermore, the exponential rise begins at a sarcomere length of ~2.0 μm in cardiac cells and ~2.3 μm in skeletal muscle fibers (Fig. 7, A and B). These lengths are consistent with a passive tension mechanism in which unraveling of titin occurs only after the elastic titin filament is completely straight. The two-stage model of passive tension development proposed is schematically depicted in Fig. 9.

The model of Fig. 9 also hypothesizes that during shortening to below the slack length titin develops a restoring force that brings sarcomeres back to the slack length. This proposal is based on our observation that in severely shortened sarcomeres the T12 epitope remains 80–100 nm away from the Z-line (Fig. 6). Furthermore, in recent preliminary studies we found that, unlike T12, Ti-102 abuts the Z-line in sarcomeres of ~1.6 μm length (Trombitás and Granzier, unpublished observations). It seems likely therefore that during sarcomere shortening below the slack length the ends of the thick filaments move past the T12 epitope toward the Z-line, straightening the highly folded elastic titin segment (Fig. 9 D), just as occurs when the sarcomere length increases beyond slack (Fig. 9 B). Straightening of titin, both below and above the slack length, and unraveling of titin domains at a length longer than ~2.0 μm occur over the working range of sarcomeres in the heart (~1.8–2.4 μm; Rodriguez et al., 1992) and are likely to be physiologically important.

REFERENCES

Brady, A. 1991. Cardiac myocyte mechanics. *Physiol. Rev.* 71:413–424.

Erickson, H. 1994. Reversible unfolding of fibronectin type III and immunoglobulin domains provides the structural basis for stretch and elasticity of titin and fibronectin. *Proc. Natl. Acad. Sci. USA.* 91:10114–10118.

Florey, P. 1969. Statistical Mechanics of Chain Molecules. John Wiley & Sons, New York.

Franzini-Armstrong, C. 1970. Details of the I-band structure as revealed by the localization of ferritin. *Tissue Cell.* 2:327–338.

Fritz, J., J. Wolff, and M. Greaser. 1993. Characterization of a partial cDNA clone encoding porcine skeletal muscle titin: comparison with rabbit and mouse skeletal muscle titin sequences. *Comp. Biochem. Physiol.* 105B:357–360.

Fulton, A., and W. Isaacs. 1991. Titin, a huge, elastic sarcomeric protein with a probable role in morphogenesis. *BioEssays.* 13:157–161.

Funatsu, T., E. Kono, H. Higuchi, S. Kimura, S. Ishiwata, T. Yoshioka, K. Maruyama, and S. Tsukita. 1993. Elastic filaments in situ in cardiac muscle: deep-etch replica analysis in combination with selective removal of actin and myosin filaments. *J. Cell Biol.* 120:711–724.

Fürst, D., M. Osborn, M. Nave, and K. Weber. 1988. The organization of titin filaments in the half-sarcomere revealed by monoclonal antibodies in immunoelectron microscopy: a map of ten nonrepetitive epitopes starting at the Z-line extends close to the M-line. *J. Cell Biol.* 106:1563–1572.

Granzier, H. L. M., and T. Irving. 1995. Passive tension in cardiac muscle: contribution of collagen, titin, microtubules and intermediate filaments. *Biophys. J.* 68:1027–1044.

Granzier, H. L. M., and K. Wang. 1993a. Interplay between passive tension and strong and weak cross-bridges in insect asynchronous flight muscle: a functional dissection by gelsolin mediated thin filament removal. *J. Gen. Physiol.* 101:235–270.

Granzier, H. L. M., and K. Wang. 1993b. Gel electrophoresis of giant proteins: solubilization and silver staining of titin and nebulin from single muscle fiber segments. *Electrophoresis.* 14:56–64.

Granzier, H. L. M., and K. Wang. 1993c. Passive tension and stiffness of vertebrate skeletal muscle and insect flight muscle: the contribution of weak crossbridges and elastic filaments. *Biophys. J.* 65:2141–2159.

Higuchi, H. 1992. Changes in contractile properties with selective digestion of connectin (titin) in skinned fibers of frog skeletal muscle. *J. Biochem.* 111:291–295.

Higuchi, H., N. Nakauchi, K. Maruyama, and S. Fujime. 1993. Characterization of β-connectin (titin 2) from striated muscle by dynamic light scattering. *Biophys. J.* 65:1906–1915.

Higuchi, H., T. Suzuli, S. Kimura, S. Yoshioka, K. Maruyama, and Y. Umazuma. 1992. Localization and elasticity of connectin filaments in skinned frog muscle fibers subjected to partial depolymerization of thick filaments. *J. Muscle Res. Cell Motil.* 13:285–294.

Hill, C., and K. Weber. 1986. Monoclonal antibodies distinguish titins from heart and skeletal muscle. *J. Cell Biol.* 102:1099–1108.

Horowits, R. 1992. Passive force generation and titin isoforms in mammalian skeletal muscle. *Biophys. J.* 61:392–398.

Horowits, R., E. S. Kempner, M. E. Bisher, and R. Podolsky. 1986. A physiological role for titin and nebulin in skeletal muscle. *Nature.* 323:160–164.

Horowits, R., K. Maruyama, and R. Podolsky. 1989. Elastic behavior of connectin filaments during thick filament movement in activated skeletal muscle. *J. Cell Biol.* 109:2169–2176.

Horowits, R., and R. Podolsky. 1987. The positional stability of thick filaments in activated skeletal muscle: evidence for the role of titin filaments. *J. Cell Biol.* 105:2217–2223.

Hu, D., S. Kimura, and K. Maruyama. 1986. Sodium dodecyl sulfate gel electrophoresis studies of connectin-like high molecular weight proteins of various types of vertebrate and invertebrate muscles. *J. Biochem.* 99:1485–1492.

Itoh, Y., T. Suzuki, S. Kimura, K. Ohashi, H. Higuchi, H. Sawada, T. Shinizu, M. Shibata, and K. Maruyama. 1988. Extensible and less-extensible domains of connectin filaments in stretched vertebrate skeletal muscle sarcomeres as detected by immunofluorescence and immunoelectron microscopy using monoclonal antibodies. *J. Biochem.* 104:504–508.

Jin, J.-P. 1995. Cloned rat cardiac titin class I and class II motifs: expression, purification, characterization, and interaction with F-actin. *J. Biol. Chem.* 270(12):6908–6916.

Kruger, M., J. Wright, and K. Wang. 1991. Nebulin as a length regulator of thin filaments of vertebrate skeletal muscles: correlation of thin filament length, nebulin size, and epitope profile. *J. Cell Biol.* 115:97–107.

Kurzban, G., and K. Wang. 1988. Giant polypeptides of skeletal muscle titin: sedimentation equilibrium in guanidine hydrochloride. *Biochem. Biophys. Res. Commun.* 150:1155–1161.

Kyhse-Anderson, J. 1984. Electroblotting of multiple gels: a simple apparatus without buffer tank for rapid transfer of proteins from polyacrylamide to nitrocellulose. *J. Biochem. Biophys. Methods.* 10:203–209.

Labeit, S., D. Barlow, M. Gautel, T. Gibson, C. Hsieh, U. Francke, K. Leonard, J. Wardale, A. Whiting, and J. Trinick. 1990. A regular pattern

of two types of 100-residue motif in the sequence of titin. *Nature.* 345:273–276.

Labeit, S., M. Gautel, A. Lackey, and J. Trinick. 1992. Towards a molecular understanding of titin. *EMBO J.* 11:1711–1716.

Linke, W., V. Popov, and G. Pollack. 1994. Passive and active tension in single cardiac myofibrils. *Biophys. J.* 67:782–792.

Maruyama, K. 1986. Connectin an elastic filamentous protein of striated muscle. *Int. Rev. Cytol.* 104:81–114.

Maruyama, K. 1994. Connectin, an elastic protein of striated muscle. *Biophys. Chem.* 50:73–85.

Maruyama, K., T. Endo, H. Kume, Y. Kawamura, N. Kanzawa, Y. Nakauchi, S. Kimura, and K. Maruyama. 1993. A novel domain sequence of connectin localized at the I band of skeletal muscle sarcomeres: homology to neurofilament subunits. *Biochem. Biophys. Res. Commun.* 194:1288.

Maruyama, K., S. Kimura, H. Yoshidomi, H. Sawada, and M. Kikuchi. 1984. Molecular size and shape of β-connectin, an elastic protein of striated muscle. *J. Biochem.* 95:1423–1433.

Page, S., L. McCallister, and B. Power. 1971. Stereological measurements of cardiac ultrastructures implicated in excitation-contraction coupling. *Proc. Natl. Acad. Sci. USA.* 68:1464–1466

Pan, K., S. Damodaran, and M. Greaser. 1994. Isolation and characterization of titin T1 from bovine cardiac muscle. *Biochemistry.* 33:8255–8261.

Pierobon-Bormioli, S., R. Betto, and G. Salviati. 1989. The organization of titin (connectin) and nebulin in the sarcomeres: an immunocytolocalization study. *J. Muscle Res. Cell Motil.* 10:446–456.

Rodriguez, E., W. Hunter, M. Royce, M. Leppo, A. Douglas, and H. Weisman. 1992. A method to reconstruct myocardial sarcomere lengths and orientations at transmural sites in beating canine hearts. *Am. J. Physiol.* 263:H293–H306.

Roos, K., and A. Brady. 1989. Stiffness and shortening changes in myofilament-extracted rat cardiac myocytes. *Am. J. Physiol.* 256:H539–H551.

Sambrook, J., E. F. Fritsch, and T. Maniatis. 1989. Molecular Cloning. Cold Spring Harbor Laboratory Press, Cold Spring Harbor, NY.

Sebestyén, M., J. Wolff, and M. Greaser. 1995. Characterization of a novel 5.4-kb cDNA fragment coding for the amino-terminal region of rabbit cardiac titin. *Biophys. J.* 68:A65.

Swerdlow, P., D. Finley, and A. Varshavsky. 1986. Enhancement of immunoblot sensitivity by heating of hydrated filters. *Ann. Biochem.* 156:147–153.

Suzuki, J., S. Kimura, and K. Maruyama. 1993. Connectin content in rabbit cardiac and skeletal muscle. *Int. J. Biochem.* 25:1853–1858.

Suzuki, J., S. Kimura, and K. Maruyama. 1994. Electron microscopic filament lengths of connectin and its fragments. *J. Biochem.* 116:406–410.

Trinick, J. 1991. Elastic filaments and giant proteins in muscle. *Curr. Opin. Cell Biol.* 3:112–118.

Trinick, J., P. Knight, and A. Whiting. 1984. Purification and properties of native titin. *J. Mol. Biol.* 180:331–356.

Trombitás, K., P. Baatsen, M. Kellermayer, and G. Pollack. 1991. Nature and origin of gap filaments in striated muscle. *J. Cell Sci.* 100:809–814.

Trombitás, K., and G. Pollack. 1993. Elastic properties of the titin filament in the Z-line region of vertebrate striated muscle. *J. Muscle Res. Cell Motil.* 14:416–422.

Trombitás, K., G. Pollack, J. Wright, and K. Wang. 1993. Elastic properties of the titin filaments demonstrated using a "freeze-break" technique. *Cell Motil. Cytoskeleton.* 24:274–283.

Trombitás, K., and A. Tigyi-Sebes. 1977. Fine structure and mechanical properties of insect muscle. *In* Insect Flight Muscle. R. Tregear, editor. North-Holland Publishing,, Amsterdam. 79–90.

Wang, K. 1985. Sarcomere-associated cytoskeletal lattices in striated muscle. *Cell Muscle Motil.* 6:315–369.

Wang, K., R. McCarter, J. Wright, B. Jennate, and R. Ramirez-Mitchell. 1991. Regulation of skeletal muscle stiffness and elasticity by titin isoforms. *Proc. Natl. Acad. Sci. USA.* 88:7101–7109.

Wang, K., R. McCarter, J. Wright, B. Jennate, and R. Ramirez-Mitchell. 1993. Viscoelasticity of the sarcomere matrix of skeletal muscles: the titin-myosin composite filament is a dual-range molecular spring. *Biophys. J.* 64:1161–1177.

Wang, K., J. Wright, and R. Ramirez-Mitchell. 1984a. Architecture of the titin/nebulin containing cytoskeletal lattice of the striated muscle sarcomere: evidence of elastic and inelastic domains of the bipolar filaments. *J. Cell Biol.* 99(4, Pt. 2):435a.

Wang, K., R. Ramirez-Mitchell, and D. Palter. 1984b. Titin is an extraordinarily long, flexible, and slender myofibrillar protein. *Proc. Natl. Acad. Sci. USA.* 81:3685–3689.

Wang, S.-M., and M. Greaser. 1985. Immunocytochemical studies using a monoclonal antibody to bovine cardiac titin on intact and extracted myofibrils. *J. Muscle Res. Cell Motil.* 6:293–312.

Whiting, A., J. Wardale, and J. Trinick. 1989. Does titin regulate the length of muscle thick filaments? *J. Mol. Biol.* 205:163–169.

Yoshioka, T., H. Higuchi, S. Kimura, K. Ohashi, Y. Umazume, and K. Maruyama. 1986. Effects of mild trypsin treatment on the passive tension generation and connectin splitting in stretched, skinned fibers from frog skeletal muscle. *Biomed. Res.* 7:181–186.